Available online at www.sciencedirect.com
SCIENCE DIRECT®
International Journal of Solids and Structures 43 (2006) 5909–5930
INTERNATIONAL JOURNAL OF SOLIDS and STRUCTURES
www.elsevier.com/locate/ijsolstr

Multi-wedge points and multi-wedge elements in computational mechanics: evaluation of exponent and angular distribution

A.M. Linkov, V.F. Koshelev *

Institute for Problems of Mechanical Engineering, Russian Academy of Sciences, 61 Bol'soi pr. V.O., St. Petersburg 199178, Russia

Received 17 May 2005
Available online 3 October 2005

Abstract

There is growing interest in accounting for the internal structure of a material. This interest stimulates developing tools for the accurate evaluation of fields near common vertices of structural elements, in particular, grains. This paper presents a robust method to numerically evaluate the exponent which characterizes the asymptotic behaviour of stresses and displacements at a vertex of an arbitrary number of elastic wedges. The efficiency is achieved by

(i) reduction of the problem to three-point matrix difference equations with appropriately normalized coefficients, and
(ii) finding the roots of the determinant of the matrix by specially designed iterative and search procedures. This allows us to ensure convergence and not miss closely located significant roots.

Numerical calculations for systems of two and three wedges, studied by other authors previously, show that the results agree to at least five digits. A number of new examples for three and four wedges with and without cracks reveal that the multi-wedge systems, which have more than one root generating singular stresses, are not rare; quite commonly such roots are closely located. We emphasize that this fact has important implications for the development of singular multi-wedge elements, intended to increase the accuracy of the BEM and FEM.

The appendices serve to re-examine and clarify the relation between properties of the matrix of the system, the asymptotic behaviour of stresses and displacements, and the number of stress intensity factors. It is shown that the necessary condition, established by Dempsey and Sinclair for the logarithmic multiplier to be present in the asymptotic formulae, is also sufficient.

Keywords: Plane elasticity; Multi-wedge points; Asymptotics; Singular boundary elements

* Corresponding author. Tel.: +7 812 372 38 43; fax: +7 812 321 47 71.
E-mail addresses: linkoval@prz.rzeszow.pl (A.M. Linkov), vadimkoshelev@yandex.ru (V.F. Koshelev).

0020-7683/$ - see front matter © 2005 Elsevier Ltd. All rights reserved.
doi:10.1016/j.ijsolstr.2005.08.005

1. Introduction

Modern computational mechanics tends to account for such elements of internal structure of a medium as interacting grains, inclusions, cracks, and pores. This increases interest in fields around so-called singular points. In 2D, these are kink points of an external boundary (Fig. 1a); points where boundary conditions change, for instance, from prescribed tractions to displacements (Fig. 1b); return points, such as an open (Fig. 1c) or closed (Fig. 1d) crack tip; and points which are common vertices of a number of grains, either within a body (Fig. 1e), or adjusted on the boundary of a body (Fig. 1f). In 3D, the schemes correspond to a cross-section normal to a rib.

The schemes of Fig. 1 obviously belong to two types of systems: open (Fig. 1a–c, f) and closed (Fig. 1d and e). The difference between these systems is that for an open system we have two external boundaries SA and SB with *boundary* conditions, whereas in a closed system there are no such boundaries and we have contacts with *contact* conditions. Certainly, since in a bi-harmonic problem we need to satisfy two contact conditions, there may be systems with the angle $\Theta = 2\pi$, which being closed with respect to one of the conditions, are open with the respect to the other. For instance, a system with $\Theta = 2\pi$ (Fig. 1d), which has continuous normal displacement, may have discontinuous shear displacement (in particular, this is the case when the Coulomb's friction law is prescribed on the surfaces in contact). The difference between the types is not a major factor in our line of investigation, but it does influence details of calculations to be taken into account.

We will describe a singular point S of the considered types as a multi-wedge point when the number of wedges exceeds one. In 3D, in addition to such points one may also have corner points, arising at an intersection of ribs. Corner points are out of the scope of this paper; their investigation is in its early stages and a review on the subject may be found elsewhere (e.g. Nicaise and Sändig, 1999; Kolk et al., 2003).

In an elastic medium, a wedge or multi-wedge point is a source of local disturbance in stresses, strains and displacements. These quantities themselves, or at least some of their derivatives, normally tend to infinity when approaching the point. From a physical point of view, this strongly influences the mechanical behaviour of a material. On the other hand, if the singularities are not taken into account in numerical calculations, the accuracy of the results is drastically decreased. The need to account for these singularities increases with growing interest in extensions of non-local fracture criteria, like those by Neuber–Novozhilov (Neuber, 1946; Novozhilov, 1969) (see, e.g. Seweryn, 1994, 2003; Seweryn and Mroz, 1995; Dyskin, 1997; Dobroskok et al., 2005). Such criteria require accurate evaluation of average stresses over a prescribed interval, in various directions near a singular point, say, a common apex of grains.

Naturally, a vast amount of literature on the singularities exists. In fracture mechanics, research has been mostly focused on the stress intensity factors (SIFs) (see, e.g. references in Murakami, 1990). It refers to a particular case of an open system of a single wedge with the wedge angle equal to 2π. Papers on wedges with other

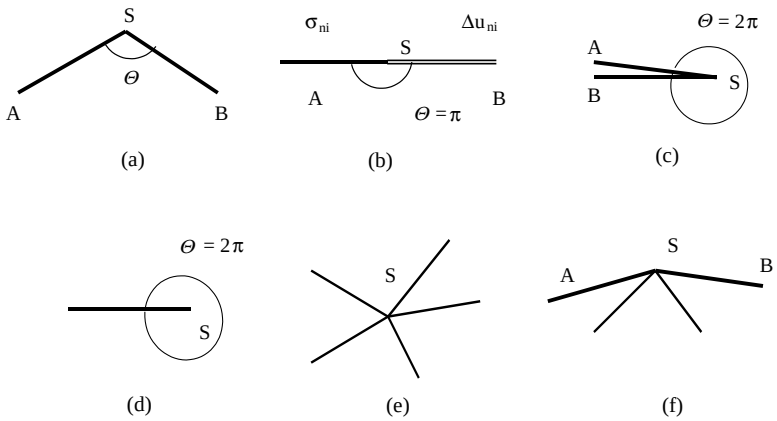

Fig. 1. Multi-wedge points in solids: (a) kink points of an external boundary; (b) points where boundary conditions change; (c) open crack tip; (d) closed crack tip; (e) common vertices of a number of grains within a body; (f) common vertices of a number of grains adjusting the boundary of a body.

angles, other number of wedges and other types of boundary conditions, although not so numerous, are still frequent. Starting from the pioneering papers by Tranter (1948) and Williams (1952, 1956), this subject has been extensively studied (e.g. Bogy, 1968, 1971; Dundurs, 1969; Kalandia, 1969; Hein and Erdogan, 1971; Rao, 1971; Cook and Erdogan, 1972; Dundurs and Lee, 1972; Theocaris, 1974; Erdogan and Gupta, 1975; Chen and Nisitani, 1993; Comninou, 1977; Dempsey and Sinclair, 1979; Dempsey, 1981) and more recently (Seweryn and Molski, 1996; Wang and Chen, 1994; Blinova and Linkov, 1995; Dempsey, 1995; Sinclair, 1998, 1999; Leblond and Frelat, 2000; Linkov et al., 2002; Noda et al., 2003; Munz, 2004). Detailed reviews can be found in Dempsey and Sinclair (1979) and Sinclair (1999).

Until 1995, no more than three wedges had been considered, since authors tend to write down an algebraic system and its determinant, defining the asymptotic behaviour, explicitly. For n wedges the determinant had order $4n$. In the case of three wedges ($n = 3$) with arbitrary angles, the system of order 12 was given in Theocaris (1974). Meanwhile, from a computational point of view, there is no need to explicitly write the characteristic determinant. All we need is a convenient rule to evaluate it. Such a rule, as shown in Blinova and Linkov (1995), is provided by an approach using the specific chain-like geometry of a multi-wedge system. In contrast with previous studies, which involved matrices of the fourth order for a single wedge, the approach by Blinova and Linkov employs matrices of the second order and reduces the problem to three-point difference equations. The latter are easily solved by the highly efficient pivotical elimination method. Having this tool for the evaluation of the characteristic determinant, one can find its roots by applying, for instance, Muller's iterations (Korn and Korn, 2000) for an arbitrary number of wedges.

The first numerical examples illustrating the method have been given in Linkov et al. (2002). They include open systems composed of a number of wedges with two sets of elastic modules and the total angle of 2π, which corresponds to an open crack terminating at a common apex of the wedges. For closed systems and systems including wedges for which matrices degenerate, the questions relating to both repeated or closely located roots and the convergence of iterations has not been studied. Meanwhile, further numerical experiments,[1] with a code based on the method of Linkov et al. (2002), have shown that these questions are of extreme importance. For instance, there are not rare multi-wedge systems with the characteristic determinant having *closely located* roots and/or *up to four* roots generating singularities in stresses. It has appeared that it is not easy to find and account for all of them. Thus, the main emphasis of the problem has shifted from obtaining a robust tool for the evaluation of the determinant to the proper use of this tool. We need to develop procedures that guarantee that none of the significant singularities are missed.

The paper tends to reach this goal. Firstly, we reexamine the starting equations of Linkov et al. (2002), presenting them in a form that prevents degeneration of the procedure in some cases. Secondly, we demonstrate arising difficulties and suggest ways to overcome them. Thirdly, the conclusions are illustrated by a number of numerical examples. In Appendix A we consider the question of repeated roots. We show that the necessary conditions established in Dempsey and Sinclair (1979), for the existence of a logarithmic multiplier in asymptotic formulae, are also sufficient. Computational implications of this fact are outlined.

2. Analysis of the asymptotic behaviour of stresses and displacements

2.1. Problem formulation

Consider a system of n wedges (open or closed) with the angles Θ_i ($i = 1, \ldots, n$). The wedges are numbered counter clockwise starting from either one that has an outer boundary for an open system (Fig. 2a), or from an arbitrary one for a closed system (Fig. 2b). The contacts are also numbered assigning the index i to the boundary between the ith and $(i + 1)$th wedges. In an open system, the outer boundary of the first wedge is assigned the index 0, while the outer boundary of the nth wedge is assigned the index n. In a closed system, the zeroth and the nth boundaries coincide. Quantities referring to the ith wedge are labelled with the superscript i;

[1] Some of the numerical results, obtained in the experiments are presented below.

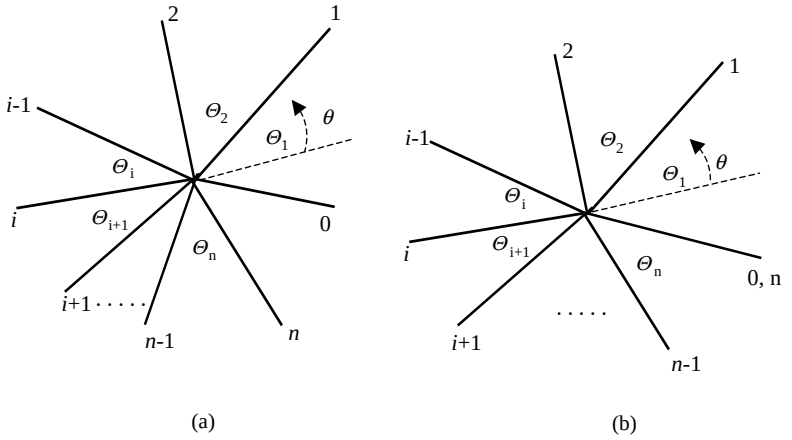

Fig. 2. Open (a) and closed (b) system of n wedges.

quantities referring to the first and the second of the wedges two boundaries are labelled with the subscripts b (bottom) and t (top), respectively. For a particular wedge, we will use local polar coordinates (r,θ), with the origin at the common apex of wedges, and the polar axis directed along the bisector, shown in Fig. 2 (by the dashed line for the first wedge).

We will focus on the bi-harmonic problem of plane strain or plane stress of elasticity theory. The harmonic problem of anti-plane strain, steady electricity, heat or ground water flow may be considered in a similar way.

For an open system, we consider prescribed tractions, or displacements, or a linear combination of their appropriate components at the outer boundaries. For a closed system, we assume prescribed dislocations (displacement discontinuities) along contacts; the dislocations are induced by external forces such as remote mechanical stresses, thermal stresses, or pore pressure, etc. The dislocations may also be present along contacts in an open system. In the case of zero dislocations we have continuous displacements through contacts.

We are interested in the asymptotic behaviour of the stresses and displacements in the vicinity of a common apex.

2.2. Mellin's transform and classification of poles

In a plane elasticity problem for wedges, Mellin's transform of stresses and displacements is used in the form:

$$\sigma_{kj}(\rho,\theta)=\int_0^\infty r^2\sigma_{kj}(r,\theta)r^{\rho-1}\,\mathrm{d}r,\quad u_k(\rho,\theta)=\int_0^\infty ru_k(r,\theta)r^{\rho-1}\,\mathrm{d}r. \tag{1}$$

Under definition (1), the inversion gives the physical quantities as

$$\sigma_{kj}(r,\theta)=\frac{1}{2\pi i}\int_{c-i\infty}^{c+i\infty}\sigma_{kj}(\rho,\theta)r^{-(\rho+2)}\,\mathrm{d}\rho,\quad u_k(\rho,\theta)=\frac{1}{2\pi i}\int_{c-i\infty}^{c+i\infty}u_k(\rho,\theta)r^{-(\rho+1)}\,\mathrm{d}\rho, \tag{2}$$

where c is an appropriately chosen real constant.

For a single wedge with the angle Θ, we re-write the results of Blinova and Linkov (1995) in a form that distinguishes the terms which are holomorphic in the entire complex plane ρ. In this form, equations for transformed stresses and displacements become:

$$\begin{aligned}\boldsymbol{\sigma}(\rho,\theta)=\frac{1}{\rho}\frac{1}{2}\Bigg\{&\left[\frac{1}{T^S(\rho)}\mathbf{B}^{\mathbf{S}}_{\boldsymbol{\sigma}}(\rho,\theta)\mathbf{D}^{\mathbf{S}}(\rho)+\frac{1}{T^A(\rho)}\mathbf{B}^{\mathbf{A}}_{\boldsymbol{\sigma}}(\rho,\theta)\mathbf{D}^{\mathbf{A}}(\rho)\right]\mathbf{p}_{\mathbf{t}}(\rho)\\&+\left[\frac{1}{T^S(\rho)}\mathbf{B}^{\mathbf{S}}_{\boldsymbol{\sigma}}(\rho,\theta)\mathbf{D}^{\mathbf{S}}(\rho)-\frac{1}{T^A(\rho)}\mathbf{B}^{\mathbf{A}}_{\boldsymbol{\sigma}}(\rho,\theta)\mathbf{D}^{\mathbf{A}}(\rho)\right]\mathbf{G}\mathbf{p}_{\mathbf{b}}(\rho)\Bigg\},\end{aligned} \tag{3}$$

$$\mathbf{u}(\rho,\theta)=\frac{1}{2\mu\rho(\rho+1)}\frac{1}{2}\left\{\left[\frac{1}{T^S(\rho)}\mathbf{B}^{\mathbf{S}}_{\mathbf{u}}(\rho,\theta)\mathbf{D}^{\mathbf{S}}(\rho)+\frac{1}{T^A(\rho)}\mathbf{B}^{\mathbf{A}}_{\mathbf{u}}(\rho,\theta)\mathbf{D}^{\mathbf{A}}(\rho)\right]\mathbf{p}_{\mathbf{t}}(\rho)\right.$$
$$\left.+\left[\frac{1}{T^S(\rho)}\mathbf{B}^{\mathbf{S}}_{\mathbf{u}}(\rho,\theta)\mathbf{D}^{\mathbf{S}}(\rho)-\frac{1}{T^A(\rho)}\mathbf{B}^{\mathbf{A}}_{\mathbf{u}}(\rho,\theta)\mathbf{D}^{\mathbf{A}}(\rho)\right]\mathbf{G}\mathbf{p}_{\mathbf{b}}(\rho)\right\},\tag{4}$$

where

$$\boldsymbol{\sigma}(\rho,\theta)=\begin{pmatrix}\sigma_{\theta\theta}(\rho,\theta)\\ \sigma_{r\theta}(\rho,\theta)\\ \sigma_{rr}(\rho,\theta)\end{pmatrix},$$
$$\mathbf{u}(\rho,\theta)=\begin{pmatrix}u_\theta(\rho,\theta)\\ u_r(\rho,\theta)\end{pmatrix},$$
$$T^S(\rho)=(\rho+1)\sin\Theta+\sin(\rho+1)\Theta,$$
$$T^A(\rho)=(\rho+1)\sin\Theta-\sin(\rho+1)\Theta,$$

and $\mathbf{B}^{\mathbf{S}}_{\boldsymbol{\sigma}}$, $\mathbf{B}^{\mathbf{S}}_{\mathbf{u}}$, $\mathbf{D}^{\mathbf{S}}$ are matrices corresponding to symmetric loading of a wedge:

$$\mathbf{B}^{\mathbf{S}}_{\boldsymbol{\sigma}}(\rho,\theta)=\begin{pmatrix}\rho\cos\rho\theta & \rho\cos(\rho+2)\theta\\ -\rho\sin\rho\theta & -(\rho+1)(\rho+2)\sin(\rho+2)\theta\\ -\rho\cos\rho\theta & -(\rho+4)\cos(\rho+2)\theta\end{pmatrix},$$
$$\mathbf{B}^{\mathbf{S}}_{\mathbf{u}}(\rho,\theta)=\begin{pmatrix}\rho\sin\rho\theta & (\rho+2-4k)\sin(\rho+2)\theta\\ \rho\cos\rho\theta & (\rho+4k)\cos(\rho+2)\theta\end{pmatrix},$$
$$\mathbf{D}^{\mathbf{S}}(\rho)=\begin{pmatrix}(\rho+2)\sin(\rho+2)\dfrac{\Theta}{2} & \rho\cos(\rho+2)\dfrac{\Theta}{2}\\ -\rho\sin\rho\dfrac{\Theta}{2} & -\rho\cos\rho\dfrac{\Theta}{2}\end{pmatrix},\quad \mathbf{G}=\begin{pmatrix}1 & 0\\ 0 & -1\end{pmatrix}.$$

Here $\mathbf{B}^{\mathbf{A}}_{\boldsymbol{\sigma}}$, $\mathbf{B}^{\mathbf{A}}_{\mathbf{u}}$, $\mathbf{D}^{\mathbf{A}}$ are matrices corresponding to skew-symmetric loading of a wedge; they are obtained by replacing $\cos(\cdot)$ by $\sin(\cdot)$ and $\sin(\cdot)$ by $-\cos(\cdot)$ in the matrices labelled with the superscript S; the term $\mathbf{p}_{\mathbf{t}}(\rho)$ is the traction vector at the 'top' boundary of the wedge, $\mathbf{p}_{\mathbf{b}}(\rho)$ is the traction vector at the 'bottom' boundary of the wedge, such that

$$\mathbf{p}_{\mathbf{t}}=\begin{pmatrix}\sigma_{\theta\theta}(\rho,\Theta/2)\\ \sigma_{r\theta}(\rho,\Theta/2)\end{pmatrix},\quad \mathbf{p}_{\mathbf{b}}=\begin{pmatrix}\sigma_{\theta\theta}(\rho,-\Theta/2)\\ \sigma_{r\theta}(\rho,-\Theta/2)\end{pmatrix},$$

where μ is the shear modulus of the wedge; $k=1-\nu$ for plane strain, $k=1/(1+\nu)$ for plane stress and ν is the Poisson's ratio. Only $\mathbf{B}^{\mathbf{S}}_{\boldsymbol{\sigma}}$, $\mathbf{B}^{\mathbf{S}}_{\mathbf{u}}$, $\mathbf{B}^{\mathbf{A}}_{\boldsymbol{\sigma}}$ and $\mathbf{B}^{\mathbf{A}}_{\mathbf{u}}$ depend on the polar angle θ. We emphasize that T^S and the entries of $\mathbf{B}^{\mathbf{S}}_{\boldsymbol{\sigma}}$, $\mathbf{B}^{\mathbf{S}}_{\mathbf{u}}$ and $\mathbf{D}^{\mathbf{S}}$, and analogous skew-symmetric quantities labelled with "A", are holomorphic functions in any finite part of the complex plane ρ. This allows us to make conclusions on the poles which define asymptotics.

The asymptotic behaviour of physical stresses and displacements near an apex ($r\to 0$) and at infinity ($r\to\infty$) is completely defined by the poles of their transformations, respectively, to the left and to the right of the line $\operatorname{Re}\rho=-1$. Since all of the coefficients and arguments other than ρ, in (3) and (4) are real, it is clear that if ρ_k is a pole, then the conjugated value $\bar{\rho}_k$ is a pole as well. Consequently, changing ρ_k to $\bar{\rho}_k$ results in complex conjugation of the transformed stresses and displacements. Hence, in the physical plane, each pair ρ_k, $\bar{\rho}_k$ generates the term which is equal to the real part of the term generated by ρ_k doubled.

Now we classify the poles. The poles $\rho=0$ and $\rho=-1$ are well-studied: they correspond to the influence of the resultant force and the resultant moment at points far from an apex, respectively. To make conclusions on other poles, we recall that the entries of the matrices $\mathbf{B}^{\mathbf{S}}_{\boldsymbol{\sigma}}$, $\mathbf{B}^{\mathbf{S}}_{\mathbf{u}}$, $\mathbf{D}^{\mathbf{S}}$, $\mathbf{B}^{\mathbf{A}}_{\boldsymbol{\sigma}}$, $\mathbf{B}^{\mathbf{A}}_{\mathbf{u}}$ and $\mathbf{D}^{\mathbf{A}}$ are holomorphic functions, i.e. they do not produce poles. Hence, the inspection of (3), (4) shows that poles other than $\rho=0$ and $\rho=-1$ are generated by either (i) zeros of the product $T(\rho)=T^S(\rho)T^A(\rho)$ or (ii) poles of the transformed tractions $\mathbf{p}_{\mathbf{t}}(\rho)$, $\mathbf{p}_{\mathbf{b}}(\rho)$. Poles of both types are the same for stresses and displacements. These are the only two sources of singularities in stresses themselves or at least in some derivatives of stresses and displacements. We consider these types.

The zeros of $T(\rho)$ are the well-known roots of the equations $T^S(\rho)=0$ and $T^A(\rho)=0$. They correspond to eigenvalues of a *single* wedge with traction-free boundaries. For a *multi*-wedge system they do not produce singularities, although, if not properly accounted for, they may cause computational problems. To avoid such problems for a system of wedges, we will distinguish the multiplier $1/T(\rho)$ and cancel it when appropriate.

We see that only the poles of $\mathbf{p_t}(\rho)$ and $\mathbf{p_b}(\rho)$ produce singularities in the apex of a *multi*-wedge system. They themselves have two sources: (i) particular values of prescribed external actions and (ii) the geometry, elastic properties and the type (not particular values!) of boundary conditions at the outer boundaries (for open systems). The first source does not produce singularities at $r=0$ if a particular distribution of prescribed values is not singular at $r=0$. For certainty, we will assume that external loads do not have poles to the left of $\operatorname{Re}\rho=-1$. Thus we must concentrate on the poles of $\mathbf{p_t}(\rho)$ and $\mathbf{p_b}(\rho)$ arising due to the particular geometry of a multi-wedge system, physical properties of the wedges and the particular *type* of boundary conditions (for open systems). Actually, these poles produce the eigenfunctions of a problem.

Assume for simplicity that the poles are distinct. (Features of distinct and repeated poles are discussed in Appendices A and B, respectively.) We number those to the left of the line $\operatorname{Re}\rho=-1$ in order of growing $|\operatorname{Re}\rho|$. Then the residue theorem applied to (3), (4) gives the asymptotic behaviour of a typical component of stresses and displacements:

$$\sigma_{lj}=a_{0lj}+\sum_{k=1}^{\infty}a_{lj}(\rho_k)\operatorname{Re}\left[r^{-(\rho_k+2)}\right],\quad u_l=b_{0l}+\sum_{k=1}^{\infty}b_l(\rho_k)\operatorname{Re}\left[r^{-(\rho_k+1)}\right]. \tag{5}$$

As can be seen from (3) and (4), there are some dependences between the coefficients $a_{lj}(\rho_k)$ and $b_{lj}(\rho_k)$. These may be used in approximations when employing the BEM or FEM. Note, however, that the corresponding reduction of the number of unknowns is insignificant compared to the total number of unknowns used in the BEM or FEM. We see from our numerical experiments that the reduction is not worth heavy analytical and programming effort. For this reason, we will not explicitly write down the obvious but cumbersome dependences between the coefficients.

2.3. Three-point difference equation: characteristic equation

The dependence between the boundary values of the displacements $\mathbf{u_t}$, $\mathbf{u_b}$ and the tractions $\mathbf{p_t}$, $\mathbf{p_b}$ immediately follows from (3), (4) for an arbitrary wedge, that is,

$$\begin{pmatrix}\mathbf{u_t}(\rho)\\ \mathbf{u_b}(\rho)\end{pmatrix}=\frac{1}{2\mu(\rho+1)}\frac{1}{T(\rho)}\begin{pmatrix}\mathbf{R}^*_{\mathbf{tt}} & \mathbf{R}^*_{\mathbf{tb}}\\ \mathbf{R}^*_{\mathbf{bt}} & \mathbf{R}^*_{\mathbf{bb}}\end{pmatrix}\begin{pmatrix}\mathbf{p_t}\\ \mathbf{p_b}\end{pmatrix}, \tag{6}$$

where

$$\mathbf{u_t}=\begin{pmatrix}u_\theta(\rho,\Theta/2)\\ u_r(\rho,\Theta/2)\end{pmatrix},\quad \mathbf{u_b}=\begin{pmatrix}u_\theta(\rho,-\Theta/2)\\ u_r(\rho,-\Theta/2)\end{pmatrix},$$

$$\mathbf{R}^*_{\mathbf{tt}}(\rho)=\frac{1}{2}(T^A\mathbf{R}^{*\mathbf{S}}+T^S\mathbf{R}^{*\mathbf{A}}),\quad \mathbf{R}^*_{\mathbf{tb}}(\rho)=-\frac{1}{2}(T^A\mathbf{R}^{*\mathbf{S}}-T^S\mathbf{R}^{*\mathbf{A}})_1,$$

$$\mathbf{R}^*_{\mathbf{bt}}(\rho)=\frac{1}{2}(T^A\mathbf{R}^{*\mathbf{S}}-T^S\mathbf{R}^{*\mathbf{A}})',\quad \mathbf{R}^*_{\mathbf{bb}}(\rho)=-\frac{1}{2}(T^A\mathbf{R}^{*\mathbf{S}}+T^S\mathbf{R}^{*\mathbf{A}})'_1.$$

Here the subscript 1 means that the first column of a matrix has been multiplied by -1; a prime means that the first row has been multiplied by -1 and

$$\mathbf{R}^{*\mathbf{S}}(\rho)=\frac{1}{\rho}\mathbf{B}^{\mathbf{S}}_{\mathbf{u}}(\rho,\Theta/2)\mathbf{D}^{\mathbf{S}}(\rho)=\begin{pmatrix}ka_- & -T^S+kb_+\\ T^S+kb_- & -ka_+\end{pmatrix},$$

$$\mathbf{R}^{*\mathbf{A}}(\rho)=\frac{1}{\rho}\mathbf{B}^{\mathbf{A}}_{\mathbf{u}}(\rho,\Theta/2)\mathbf{D}^{\mathbf{A}}(\rho)=\begin{pmatrix}ka_+ & -T^A+kb_-\\ T^A+kb_+ & -ka_-\end{pmatrix},$$

$$a_\pm(\rho)=2(\cos\Theta\pm\cos(\rho+1)\Theta),\quad b_\pm(\rho)=2(\sin\Theta\pm\sin(\rho+1)\Theta).$$

Eq. (6) is actually the basic equation used in Blinova and Linkov (1995); here it is presented in the form distinguishing the term $1/T$, which may turn to infinity, from the starred matrices, whose entries are holomorphic functions of ρ in any finite region of the complex variable plane.

Eq. (6) holds for each wedge. We use it to meet contact conditions. We assume that the tractions are continuous across a contact. What concerns with the displacements, they may be discontinuous. In this paper we restrict ourselves only with the case when the displacement discontinuity $\mathbf{\Delta u}(r)$ is a linear function of the traction $\mathbf{p}(r)$ multiplied by r. This case includes an ideal contact ($\mathbf{\Delta u}(r) = 0$) and also the case of prescribed contact dislocations. Then in view of (1), the transformed values $\mathbf{\Delta u}(\rho)$, $\mathbf{p}(\rho)$ have the same argument ρ. For brevity, we assume for the i-th contact:

$$\mathbf{p_b^{i+1}} = \mathbf{p_t^i} = \mathbf{p^i}, \quad \mathbf{\Delta u}^i = \mathbf{u_b^{i+1}} - \mathbf{u_t^i} = \mathbf{\Delta u_0^i},$$

where $\mathbf{\Delta u_0^i}$ is a vector of prescribed dislocations. Then we arrive at the system of three-point matrix difference equations, obtained in Blinova and Linkov (1995):

$$\mathbf{A^i p^{i-1}} - \mathbf{C^i p^i} + \mathbf{B^i p^{i+1}} + \mathbf{F^i} = \mathbf{0} \quad (i = 1, \ldots, n-1),$$

where

$$\mathbf{A^i}(\rho) = \frac{1}{2\mu^i(\rho+1)}\frac{1}{T^i}(-\mathbf{R_{tb}^{*i}}), \quad \mathbf{B^i}(\rho) = \frac{1}{2\mu^{i+1}(\rho+1)}\frac{1}{T^{i+1}}\mathbf{R}_{bt}^{*i+1},$$

$$\mathbf{C^i}(\rho) = \frac{1}{\rho+1}\left(\frac{1}{2\mu^i}\frac{1}{T^i}\mathbf{R_{tt}^{*i}} - \frac{1}{2\mu^{i+1}}\frac{1}{T^{i+1}}\mathbf{R}_{bb}^{*i+1}\right), \quad \mathbf{F^i} = -\mathbf{\Delta u_0^i}.$$

To avoid computational problems with the pole $\rho = -1$ and the roots of $T^i(\rho)$, we re-write the equations as

$$\mathbf{A^{*i} p^{i-1}} - \mathbf{C^{*i} p^i} + \mathbf{B^{*i} p^{i+1}} + \mathbf{F^{*i}} = \mathbf{0} \quad (i = 1, \ldots, n-1), \tag{7}$$

where, depending on whether two successive wedges i and $i+1$ have the same angle ($\Theta^i = \Theta^{i+1}$) or different angles ($\Theta^i \neq \Theta^{i+1}$), the definition of the matrices and $\mathbf{F^{*i}}$ differs, that is, if $\Theta^i = \Theta^{i+1}$, then

$$\mathbf{A^{*i}}(\rho) = -\mathbf{R_{tb}^{*i+1}}, \quad \mathbf{B^{*i}}(\rho) = \frac{\mu^i}{\mu^{i+1}}\mathbf{R_{bt}^{*i+1}},$$

$$\mathbf{C^{*i}}(\rho) = \mathbf{R_{tt}^{*i}} - \frac{\mu^i}{\mu^{i+1}}\mathbf{R_{bb}^{*i+1}}, \quad \mathbf{F^{*i}}(\rho) = \mu^i(\rho+1)T^i\mathbf{F^i}$$

and if $\Theta^i \neq \Theta^{i+1}$, then

$$\mathbf{A^{*i}}(\rho) = -T^{i+1}\mathbf{R_{tb}^{*i}}, \quad \mathbf{B^{*i}}(\rho) = \frac{\mu^{i+1}}{\mu^i}T^i\mathbf{R_{bt}^{*i}},$$

$$\mathbf{C^{*i}}(\rho) = T^{i+1}\mathbf{R_{tt}^{i}} - \frac{\mu^i}{\mu^{i+1}}T^i\mathbf{R_{bb}^{*i+1}}, \quad \mathbf{F^{*^i}}(\rho) = \mu^i(\rho+1)T^iT^{i+1}\mathbf{F^i}$$

The entries of the matrices in (7) are holomorphic functions in any finite region of the plane ρ. To solve the system (7) for an open system we use prescribed boundary conditions at the outer boundaries ($i = 0$ and $i = n$) and for a closed system we attach cyclic conditions ($\mathbf{p^0} = \mathbf{p^n}$, $\mathbf{\Delta u^n} = \mathbf{u_b^1} - \mathbf{u_t^n} = \mathbf{\Delta u_0^0}$). Various types of boundary conditions discussed in Blinova and Linkov (1995) can be considered in the same way as used below. For certainty, in further analysis we assume that the dislocations at contacts are zero, and we consider an open system with prescribed tractions $\mathbf{p^0}$ at the boundary $i = 0$ and $\mathbf{p^n}$ at the boundary $i = n$. Then $\mathbf{\Delta u_0^i} = \mathbf{0}$, $i = 1, \ldots, n-1$ and (7) is added with the conditions:

$$-\mathbf{C^{*0} p^0} + \mathbf{F^{*0}} = \mathbf{0}, \quad -\mathbf{C^{*n} p^n} + \mathbf{F^{*n}} = \mathbf{0}, \tag{8}$$

where $\mathbf{C^{*0}} = \mathbf{C^{*n}} = \mathbf{I}$ is the unit 2×2 matrix; $\mathbf{F^{*0}} = \mathbf{p^0}$, $\mathbf{F^{*n}} = \mathbf{p^n}$. The form (8) is similar to (7) what simplifies using standard formulae of the Gauss pivotal elimination. As an alternative, when convenient, we will substitute the prescribed $\mathbf{p^0}$ into (7) for $i = 1$, the prescribed $\mathbf{p^n}$ for $i = n-1$, and move these terms into the r.h.s. of (7). Then system (7) becomes a system for $2(n-1)$ unknown tractions at contacts $i = 1, \ldots, n-1$.

We recall that we have assumed that the poles of the transformed external loads $\mathbf{p^0}$ and $\mathbf{p^n}$ are located to the right of $\mathrm{Re}\,\rho = -1$. We denote by $D(\rho)$ the determinant of the system (7) and (8). Then applying Cramer's rule to the system implies that only the roots of the characteristic equation

$$D(\rho) = 0, \tag{9}$$

located to the left of $\mathrm{Re}\,\rho = -1$, produce the poles of $\mathbf{p^i}(\rho)$ $(i = 1, \ldots, n-1)$ with $\mathrm{Re}\,\rho < -1$. As is clear from the first equation of (5), these roots of (9) generate physically significant singularities in stresses and/or their derivatives at the apex $r = 0$. Precisely, the roots in the strip $-2 < \mathrm{Re}\,\rho < -1$ generate singularities in stresses and, consequently, in their derivatives; those with $-3 < \mathrm{Re}\,\rho < -2$ generate singularities in first and higher-order derivatives of stresses; those with $-4 < \mathrm{Re}\,\rho < -3$ in the second and higher-order derivatives and so on. Similar conclusions follow from the second equation of (5) for the first and higher-order derivatives of displacements. The roots in the strip $-2 < \mathrm{Re}\,\rho < -1$, providing singularities in the stresses themselves, are of the prime interest for our study.

3. Numerical procedures

3.1. Muller's iterations

For a given complex number ρ, Eqs. (6)–(8) allow one to easily evaluate the characteristic determinant $D(\rho)$ for a system with an arbitrary number of wedges, the arbitrary wedge angles and the elastic parameters. This means that one can use iterative procedures when solving the characteristic Eq. (9). As mentioned, we are mostly interested in the roots ρ_j $(j = 1, \ldots)$ of (9) within the strip $-2 \leqslant \mathrm{Re}\,\rho_j < -1$. For further discussion, it is convenient to use $\lambda_j = 2 + \rho_j$ instead of ρ_j, since stresses and displacements, defined by the root, behave as $\sigma = A_j r^{-\lambda_j}$ and $u = B_j r^{1-\lambda_j}$, respectively. Consequently the strip becomes $0 < \mathrm{Re}\,\lambda_j < 1$.

The root with the greatest real part less than 1 is the most significant as it produces the strongest physically admissible singularity in stresses. Meanwhile, as it appears, there may be other roots in the strip and they also must be accounted for.

In order to find the roots which in general are complex numbers, Muller's iterations may be used. The procedure is as follows. We let three successive approximate values of a root be denoted by τ_{k-2}, τ_{k-1}, τ_k $(k = 1, 2, \ldots)$. Then the second degree interpolation polynomial $D_*(\lambda)$, approximating $D(\lambda)$, is:

$$D_*(\lambda) = D(\tau_k) + (\lambda - \tau_k)D(\tau_k, \tau_{k-1}) + (\lambda - \tau_k)(\lambda - \tau_{k-1})D(\tau_k, \tau_{k-1}, \tau_{k-2}),$$

where $D(\tau_k, \tau_{k-1}) = [D(\tau_k) - D(\tau_{k-1})]/(\tau_k - \tau_{k-1})$; $D(\tau_k, \tau_{k-1}, \tau_{k-2}) = [D(\tau_k, \tau_{k-1}) - D(\tau_{k-1}, \tau_{k-2})]/(\tau_k - \tau_{k-2})$. Using the notation $z = \lambda - \tau_k$, the equation $D_*(\lambda) = 0$ becomes

$$az^2 + bz + c = 0, \tag{10}$$

where $a = D(\tau_k, \tau_{k-1}, \tau_{k-2})$, $b = D(\tau_k, \tau_{k-1}) + (\tau_k - \tau_{k-1})D(\tau_k, \tau_{k-1}, \tau_{k-2})$, $c = D(\tau_k)$. The solution of (10) gives (in general) two complex roots $z^{(1)}$, $z^{(2)}$ and consequently, the roots $\lambda^{(1)}$, $\lambda^{(2)}$. As a new approximation of the root of (9), we choose between $\lambda^{(1)}$, $\lambda^{(2)}$ whichever one that is closer to τ_k: $\tau_{k+1} = \min(|\tau_k - \lambda^{(1)}|, |\tau_k - \lambda^{(2)}|)$. Then the procedure is repeated for τ_{k-1}, τ_k, τ_{k+1}. We proceed until we reach the prescribed accuracy.

3.2. Initiation: procedures to distinguish roots

3.2.1. Initiation

The procedure described is simple and robust. The main problem is to properly initiate this procedure in the considered strip. For each of the (possibly several) roots we need to prescribe three starting values τ_{-1}, τ_0, τ_1 sufficiently close to the root, so as to avoid divergence and guarantee convergence to this particular root, rather than to another one. Thus, we actually have two problems: (i) to obtain at least one root; (ii) to check whether there are other roots in the strip and if there are, to find them. To solve these problems, we use two approaches, which being combined, complement each other.

3.2.2. Step-by-step approach for finding a root

Consider an arbitrary system of n wedges. Let us have a root for another system, where this second system resembles the first in some ways. Call the second system 'approximate'. For clarity, assume that the considered n-wedge system is open with prescribed tractions at the external boundaries, and take an 'approximate' system to be the system with the same geometry as the considered system, but comprising of wedges having invariable elastic properties: $\mu_{a1} = \mu_{a2} = \cdots = \mu_{an}$, $\nu_{a1} = \nu_{a2} = \cdots = \nu_{an}$. Then we actually have a single homogeneous wedge, for which the roots are well known. We take one of these roots, for instance, the one with the greatest real part λ_{a0} ($\lambda_{a0} < 1$). We also take two close values $\lambda_{a0} - \delta$ and $\lambda_{a0} + \delta$, where δ is a small number ($\delta \sim 10^{-1}$–10^{-2}). Now we slightly change the elastic properties of the approximate system by taking them closer to those of the considered system. Then we obtain a new 'approximate' system with unknown roots, in which the values $\tau_{-1} = \lambda_{a0} - \delta$, $\tau_0 = \lambda_{a0}$, $\tau_1 = \lambda_{a0} + \delta$ present a good starting approximation to find a root using Muller's iterations. By using the iterations, we obtain the root λ_{a1} of the new approximate system. We again slightly change the properties of the approximate system, taking them closer to those of the considered system and use the values $\tau_{-1} = \lambda_{a1} - \delta$, $\tau_0 = \lambda_{a1}$, $\tau_1 = \lambda_{a1} + \delta$ to find the root λ_{a2} for the new approximate system, and so on. In this way, we arrive at the system coinciding with that under consideration, and obtain its root in a finite number of changes of the elastic properties.

3.2.3. Tracing changes of the determinant

The approach described always gives us one root with high accuracy. It would be sufficient if there were no other significant roots. Unfortunately and quite commonly, there exist a number of roots in the strip, and some of them are close to each other. To avoid missing these, we suggest tracing the changes of the characteristic determinant in the strip along the lines $\mathrm{Im}\,\lambda = \mathrm{const}$. The graphs of the absolute value of the determinant, normalized by its maximal value, give a clear visual picture which provides information on the areas where roots are located.

As examples, Figs. 3 and 4 show the graphs $|D(\lambda)|/\max|D|$ for an open system of three wedges with $\Theta_1 = \Theta_3 = \pi/4$; $\Theta_2 = 3\pi/2$; $\nu_1 = \nu_2 = \nu_3 = 0.30$; $\mu_1 = \mu_3 = 10\mu_2$. The graphs are plotted for three values of $\mathrm{Im}\,\lambda$: 0.00, 0.02 and 0.04. The graphs of Fig. 3 correspond to 50 points in the interval $0 < \mathrm{Re}\,\lambda < 1$; Fig. 4 corresponds to the finer mesh of 200 points in the interval. We see that even the rough mesh (Fig. 3) gives clear indication that there is a root close to $\lambda_1 \approx 0.15$; two other suspicious areas are those near the points 0.60 and 0.80, where the absolute value of the determinant rapidly decreases. The graphs of Fig. 4 confirm this

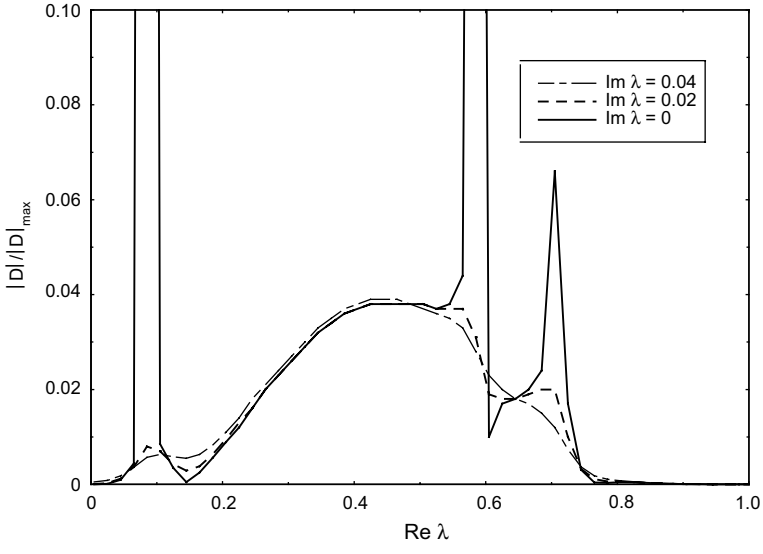

Fig. 3. Normalized absolute value of the characteristic determinant (coarse mesh: 50 points).

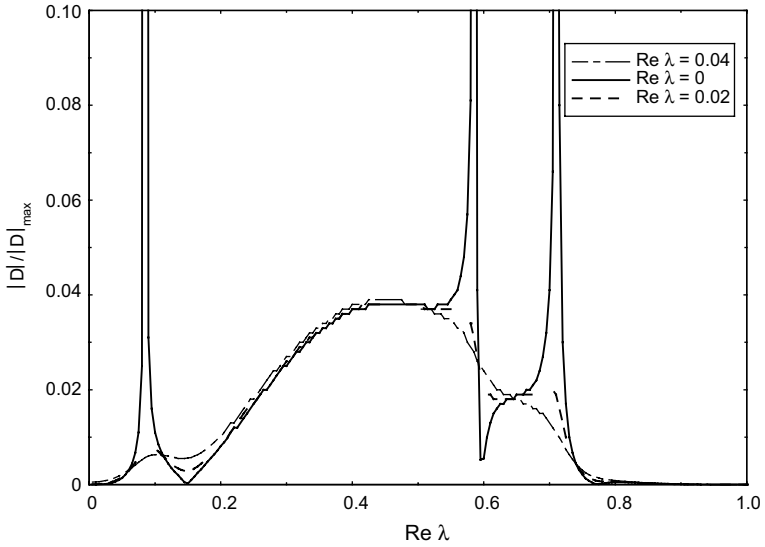

Fig. 4. Normalized absolute value of the characteristic determinant (fine mesh: 200 points).

suggestion: they clearer indicate the high possibility of roots. By taking initial approximations in the areas of possible roots and applying Muller's iterations we find the roots, to five significant digits, $\lambda_1 = 0.12917$, $\lambda_2 = 0.59840$, $\lambda_3 = 0.77176$.

Note that in order to find the root $\lambda_2 = 0.59840$, near which the determinant changes very quickly, it was necessary to choose especially close initial approximations. From our experience we could see that in such cases, the appropriate initial approximations have to satisfy the inequality $|\lambda_2 - z_0| < 0.002$; otherwise, iterations may converge to another root, or diverge.

We conclude that special attention must be paid to areas where the (negative) gradient of $|D(\lambda)|/\max|D|$ has a large absolute value. This conclusion obviously may serve for an automatic search of roots. Each of the roots found in this way, may serve to find a root of other wedge systems, by using the step-by-step approach described above.

3.3. Accuracy control

One can check the accuracy of the results by (i) comparing the results of two successive Muller's iterations and (ii) direct substitution of an obtained root into the characteristic determinant (comparing it with zero). In our study, when using the first option, we terminated the iterations when the difference between two successive values became less than the prescribed tolerance. The latter was taken as 10^{-6}–10^{-12}. With regard to the second option, in all cases, we could see that the absolute value of the determinant did not exceed 10^{-5}, normally being 10^{-8}–10^{-12}. In order to avoid an unexpected jump to a nearby root, we traced the continuity of the root as we changed the elastic modules. In suspicious cases (when rapid changes in the root occurred) we repeated the calculations for diminished δ and for smaller changes in the elastic modules within a step. (Our calculations were always carried out with double precision.)

4. Numerical results

4.1. Comparison with numerical results in the literature

Firstly, we compare the results obtained by the method described above with those for which the characteristic determinant has been previously used in the explicit form. This gives an idea of the accuracy of our calculations. Both open and closed systems are considered.

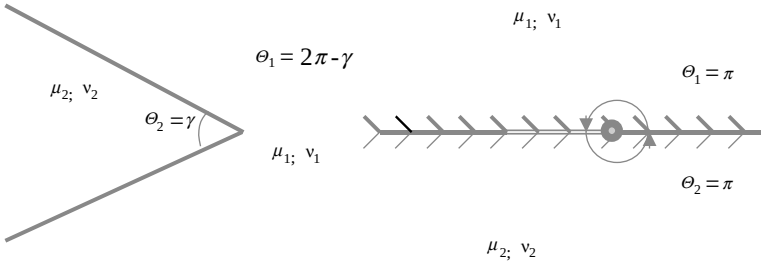

Fig. 5. Examples of closed systems: (a) two wedges; (b) half-planes with friction along a semi-infinite contact.

Table 1
Exponents for the system of two wedges (Fig. 5a)

	γ^0	30	45	60	90	120	135	150
$\mu_2/\mu_1 = 0.10$	λ_a	0.27607	0.25291	0.20591	0.06444			
	λ_s	0.21487	0.27185	0.30997	0.33986	0.30793	0.26586	0.20327
$\mu_2/\mu_1 = 10$	λ_a				0.21435	0.23852	0.21097	0.16207
	λ_s	0.31776	0.30632	0.27810	0.20189	0.12450	0.09034	0.05911

4.1.1. Closed system of two wedges (Fig. 5a)

Consider a plane composed of two wedges with the angles $\Theta_1 = 2\pi - \gamma$, $\Theta_2 = \gamma$. In this and following examples, plane strain conditions are presumed if there is no notion on plane stress. The wedges have the same Poisson ratio $\nu_1 = \nu_2 = 0.30$, while their shear modules are, in general, different. In Table 1, the exponent λ, corresponding to the strongest singularity, is presented for various angles γ and various ratios μ_2/μ_1 studied in the papers by Bogy (1971) and Noda et al. (2003).[2] The subscript s and a mark values for the symmetric and skew-symmetric cases, respectively. Empty cells of the table are those for which there are no roots in the strip $0 < \mathrm{Re}\,\lambda < 1$. The results coincide, to at least five significant figures, with those of Bogy (1971) and Noda et al. (2003).

4.1.2. System of two half-planes with friction along a semi-infinite contact (Fig. 5b)

Consider two half-planes ($\Theta_1 = \Theta_2 = \pi$) bonded along the right part of their common boundary and having friction along the left part of the boundary. The normal displacements are continuous along the entire contact. The friction law connects the tractions at the left part of the boundary, that is,

$$|\sigma_{nt}| = f|\sigma_{nn}|,$$

where f is the friction coefficient. In this case, for a particular choice of signs, the characteristic equation is (see, for example, Comninou, 1977; Leblond and Frelat, 2000):

$$ctg\lambda\pi = f|\beta|,$$

where $\beta = \frac{1}{2}\frac{\mu_2(\kappa_1-1)-\mu_1(\kappa_2-1)}{\mu_2(\kappa_1+1)-\mu_1(\kappa_2+1)}$, $\kappa_j = 3 - 4\nu_j$ for plane strain, and $\kappa_j = (3 - \nu_j)/(1 - \nu_j)$ for plane stress ($j = 1,2$).

Table 2 contains the exponent of the strongest singularity, calculated for various values of the ratio μ_2/μ_1 and the coefficient of friction. They coincide with the values of the main root of the equation. Note that in all the cases, even for very different properties of the planes, the exponents do not differ significantly from the value 0.5, which corresponds to the case of half-planes with the same elastic properties.

[2] Note that the equation for the characteristic determinant in the symmetric case is printed in Noda et al. (2003) with two misprints (cf. with correct equation in the earlier paper by Bogy (1971)).

Table 2
Exponents for the system of two half-planes (Fig. 5b)

μ_2/μ_1	1	2	4	6	8
$f = 0.10$	0.49545	0.48964	0.48519	0.48333	0.48231
$f = 0.40$	0.48183	0.45878	0.44137	0.43420	0.43029

4.1.3. Open system of three wedges (Fig. 6)

Consider an open system of three wedges with the angles γ, π and $\pi - \gamma$ ($\gamma < \pi$). In the case when the properties of the first and third wedges are the same, we have a crack terminating at the boundary of bonded half-planes. For the surfaces of the crack loaded with the prescribed tractions, the results are presented in Cook and Erdogan (1972), Erdogan and Gupta (1975) for $\gamma = \pi/2$ (Fig. 6b), and in Wang and Chen (1994) for an arbitrary γ. Note that the roots given in Erdogan and Gupta (1975) and Wang and Chen (1994) coincide to four significant digits. For certainty, we compare our results with those of the recent paper Wang and Chen, 1994. Our results, for the most contrast cases, when $\mu_2/\mu_1 = 10$ and $\mu_2/\mu_1 = 0.1$ are given in Table 3, to five digits. They are obtained for equal Poisson ratios: $\nu_1 = \nu_2 = 0.30$. The results completely coincide with those of Wang and Chen (1994) (the authors presented $1 - \lambda$). It is worth noting that in many cases listed in the table, there are two roots λ_1 and λ_2 in the strip $0 < \mathrm{Re}\,\lambda < 1$, and they are rather close to each other. We also note that, when the crack terminates at a boundary with a soft medium (inclusion), the exponents are real, except for the limiting case, when the crack is located along the boundary of the half-planes ($\gamma = 0$).

4.2. Some new numerical results

The method of Section 2 and algorithms of Section 3, having been implemented into a computer code, provide results for arbitrary multi-wedge systems. Only a few of them may be given in the present paper. Below we focus on examples, which illustrate the abilities of the code developed, and represent some structures.

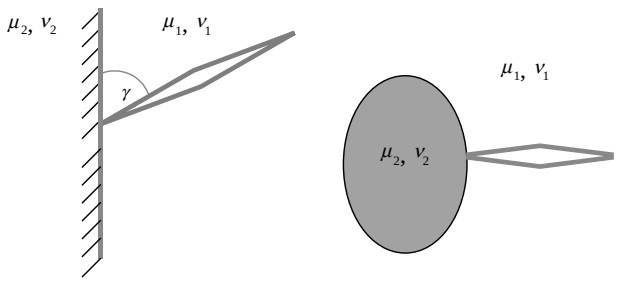

Fig. 6. Examples of open systems of three wedges: (a) a crack terminating at the boundary of bonded half-planes; (b) a particular case of a crack terminating at the boundary of two media ($\gamma = \pi/2$).

Table 3
Exponents for the open system of three wedges (Fig. 6a)

	γ^0	0	15	30	45	60	75	90
$\mu_2/\mu_1 = 10$	λ_1	0.50000+ i*0.09377	0.45778+ i*0.09674	0.40417+ i*0.08509	0.33910+ i*0.02026	0.37207	0.34788	0.30333
	λ_2	–	–	–	–	0.20658	0.24201	–
$\mu_2/\mu_1 = 0.1$	λ_1	0.50000+ i*0.09377	0.73172	0.78140	0.79459	0.79188	0.77741	0.75144
	λ_2		0.52756	0.54956	0.59774	0.65781	0.71141	–

4.2.1. Four grains with a common apex (Fig. 7)

Consider a closed system of four wedges with the same angle $\Theta_1 = \Theta_2 = \Theta_3 = \Theta_4 = \pi/2$. This could represent the vicinity of the common apex of four grains. Assume that $\mu_1 = \mu_3$ and $\mu_2 = \mu_4$. For the Poisson ratio we take $\nu_1 = \nu_2 = \nu_3 = \nu_4 = 0.3$, as above. Table 4 contains the roots in the strip $0 < \mathrm{Re}\,\lambda < 1$. We see that there are two roots; it is especially remarkable that, for sufficiently large ratio μ_2/μ_1, the both roots generate rather strong singularities and the difference between them is small. Hence, both roots are significant, and special attention must be paid to properly account for their closeness when developing singular multi-wedge boundary elements.

4.2.2. Crack symmetrically emanating from the corner of a square inclusion outside square (Fig. 8a)

In this case we have an open system of three wedges with the angles $\Theta_1 = \Theta_3 = 3\pi/4$, $\Theta_2 = \pi/2$. Table 5 contains roots for the crack tip at the corner of the inclusion for various ratios $\mu_{\mathrm{inc}}/\mu_{\mathrm{m}}$ of the shear moduli of the inclusion and the matrix. The Poisson ratio is the same $\nu_{\mathrm{inc}} = \nu_{\mathrm{m}} = 0.3$. We see that all the roots are real. For a sufficiently rigid inclusion, when $\mu_{\mathrm{inc}}/\mu_{\mathrm{m}} > 2$, there exist at least three roots in the strip $0 < \mathrm{Re}\,\lambda < 1$; when $\mu_{\mathrm{inc}}/\mu_{\mathrm{m}} = 10$ there are *four* such roots. For compliant inclusions ($\mu_{\mathrm{inc}}/\mu_{\mathrm{m}} < 1$), there are two roots.

4.2.3. Crack symmetrically emanating from the corner of a square inclusion inside the square (Fig. 8b)

In this case we have an open system of three wedges with the angles $\Theta_1 = \Theta_3 = \pi/4$, $\Theta_2 = 3\pi/2$. As above, $\nu_{\mathrm{inc}} = \nu_{\mathrm{m}} = 0.3$. The results are given in Table 6. All the roots are real. As a rule there are two roots in the strip $0 < \mathrm{Re}\,\lambda < 1$.

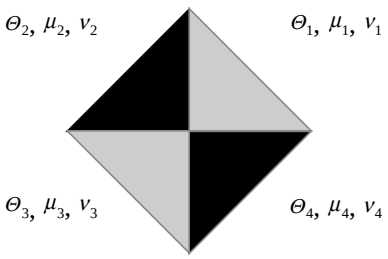

Fig. 7. Closed system of four wedges with the same angles.

Table 4
Exponents for the closed system of four grains with a common apex (Fig. 7)

μ_2/μ_1	2.0	3.0	4.0	5.0	6.0	7.0	8.0	10.0
λ_1	0.20628	0.32320	0.40033	0.45602	0.49863	0.53258	0.56046	0.60392
λ_2	0.06503	0.14918	0.21929	0.27608	0.32265	0.36154	0.39457	0.44787

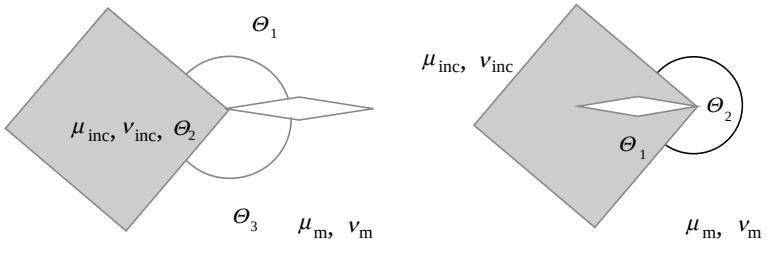

Fig. 8. Crack emanating from the corner of a square inclusion: (a) outside the inclusion; (b) inside the inclusion.

Table 5
Exponents for the square inclusion and outside crack emanating from the corner (Fig. 8a)

μ_{inc}/μ_m	0.10	0.20	0.50	2.0	4.0	6.0	8.0	10.0
λ_1	0.77415	0.69791	0.58298	0.45709	0.42899	0.41751	0.41108	0.40691
λ_2	0.74349	0.66500	0.56166	0.43029	0.39022	0.37486	0.36796	0.36461
λ_3				0.06447	0.11897	0.14302	0.15666	0.16547
λ_4								0.03213

Table 6
Exponents for the square inclusion and inside crack emanating from the corner (Fig. 8b)

μ_{inc}/μ_m	0.10	0.20	0.25	0.50	2.0	4.0	6.0	8.0	10.0
λ_1	0.46196	0.46779	0.47050	0.48235	0.52281	0.55013	0.56913	0.58474	0.59840
λ_2	0.19854	0.26732	0.29454	0.39218	0.60254	0.68828	0.72913	0.75423	0.77176
λ_3					0.05559	0.09450	0.11113	0.12165	0.12917

4.2.4. Crack symmetrically emanating from the corner of a composite inclusion outside the inclusion (Fig. 9a)

This case differs from that of 4.2.2 in that now the square inclusion is composed of two triangular parts with, in general, different properties. We have four wedges with the angles $\Theta_1 = \Theta_4 = 3\pi/4$, $\Theta_2 = \Theta_3 = \pi/4$. Table 7 contains results in the case when the inclusion is *rigid* ($\mu_2/\mu_1 = 10$). The roots are given for various values of μ_3/μ_2. The Poisson's ratio of all wedges is the same $\nu_1 = \nu_2 = \nu_3 = \nu_4 = 0.30$. In the case considered, if the properties of the triangular parts differ significantly ($\mu_3/\mu_2 < 0.5$), then there are two roots, and they are complex with an imaginary part that is significantly less than the real part. The imaginary part tends to zero when $\mu_3/\mu_2 \to 0.5$. For triangles with close values of the shear modulus ($\mu_3/\mu_2 > 0.5$), there are three roots, and all of them are real.

The results for a *compliant* inclusion ($\mu_2/\mu_1 = 0.1$) are given in Table 8. In this case we have two closely located roots with strong singularities (λ_1, $\lambda_2 > 0.66$), and they are real.

4.2.5. Crack symmetrically emanating from the corner of a composite inclusion inside the inclusion (Fig. 9b)

Now we have $\Theta_1 = \Theta_3 = \pi/4$, $\Theta_2 = 3\pi/4$. For a rigid inclusion ($\mu_1/\mu_2 = 10$) the roots are given in Table 9. All roots are real, and the two largest are close to each other; the third is notably smaller. The values of the roots grow with increasing ratio μ_3/μ_2.

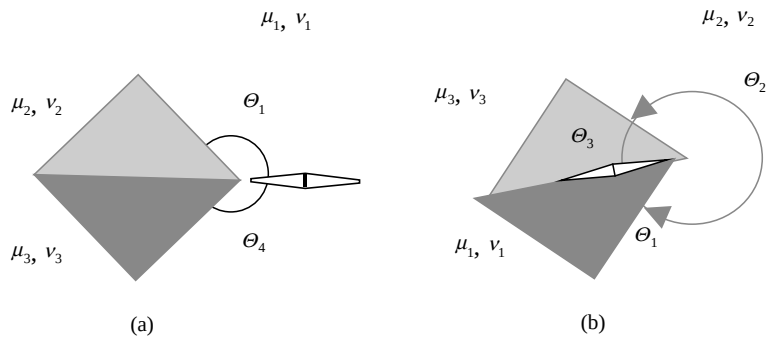

Fig. 9. Crack emanating from the corner of a composite inclusion: (a) outside the inclusion; (b) inside the inclusion.

Table 7
Exponents for the rigid composite inclusion with a crack (Fig. 9a)

μ_3/μ_2	0.10	0.20	0.30	0.40	0.50	0.60	0.70	0.80
λ_1	0.47267+ i*0.04450	0.42780+ i*0.03462	0.41000+ i*0.02258	0.40074+ i*0.0090	0.38258	0.37424	0.36968	0.36701
λ_2	0.13467	0.14073	0.14548	0.14953	0.15307	0.15619	0.15894	0.16138
λ_3					0.40794	0.40927	0.40912	0.40852

Table 8
Exponents for the compliant composite inclusion with a crack (Fig. 9a)

μ_3/μ_2	2.0	3.0	4.0	5.0	6.0	7.0	8.0	9.0
λ_1	0.74890	0.74096	0.73740	0.73558	0.73462	0.73416	0.73400	0.73403
λ_2	0.70627	0.68766	0.67744	0.67145	0.66782	0.66562	0.66430	0.66356

Table 9
Exponents for the rigid composite inclusion and outside crack (Fig. 9b)

μ_3/μ_2	0.10	0.20	0.30	0.40	0.50	0.60	0.70	0.80	0.90
λ_1	0.64565	0.68585	0.71138	0.72846	0.74067	0.74986	0.75706	0.76288	0.76769
λ_2	0.54179	0.56068	0.56918	0.57504	0.57984	0.58408	0.58798	0.59164	0.59510
λ_3	0.04621	0.08602	0.10186	0.11049	0.11602	0.11995	0.12296	0.12501	0.12741

For a compliant inclusion ($\mu_1/\mu_2 = 0.1$), there are two roots (see Table 10). They are real, and the largest grows slightly with increasing ratio μ_3/μ_2.

4.2.6. Open system of five wedges (Fig. 10)

Four grains, with a crack emanating from their common apex, present an open system of five wedges. Take $\Theta_1 = \Theta_5 = \pi/4,\ \Theta_2 = \Theta_3 = \Theta_4 = \pi/2;\ \mu_5 = \mu_1 = \mu_3,\ \mu_2 = \mu_4;\ \nu_j = 0.3\ (j = 1, \ldots, 5)$. First, consider the case when the grain containing the crack is rigid ($\mu_1/\mu_2 > 1$). The results, given in Table 11, show that, in this case,

Table 10
Exponents for the compliant composite inclusion and outside crack (Fig. 9b)

μ_3/μ_2	2.0	3.0	4.0	5.0	6.0	7.0	8.0	9.0
λ_1	0.46512	0.46847	0.47200	0.47569	0.47952	0.48345	0.48745	0.49148
λ_2	0.23517	0.26451	0.28828	0.30773	0.32379	0.33716	0.34837	0.35784

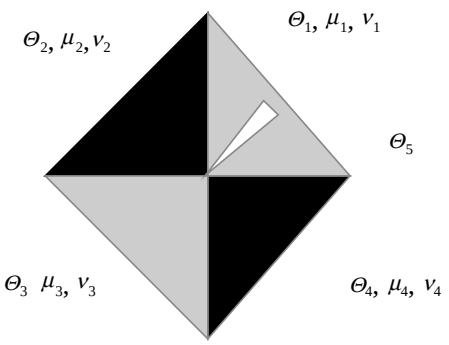

Fig. 10. Crack emanating from the common apex of four grains.

Table 11
Exponents for a crack emanating from the common apex of four grains (Fig. 10); the crack is in a rigid grain

μ_1/μ_2	2.0	3.0	4.0	5.0	6.0	7.0	8.0	9.0	10.0
λ_1	0.55012	0.59130	0.62290	0.64787	0.66823	0.68526	0.69980	0.71241	0.72351
λ_2	0.49677	0.52419	0.55538	0.58403	0.60920	0.63059	0.64925	0.66552	0.67983
λ_3	0.13273	0.20072	0.24083	0.26869	0.29063	0.30935	0.32610	0.34151	0.35592
λ_4					0.02432	0.07276	0.11412	0.15012	0.18192

Table 12
Exponents for a crack emanating from the common apex of four grains (Fig. 10); the crack is in a soft grain

μ_1/μ_2	0.5	0.(3)	0.25	0.2	0.1(6)	0.14286	0.125	0.(1)	0.1
λ_1	0.55249	0.59673	0.63085	0.65777	0.67961	0.69775	0.71313	0.72637	0.73793
λ_2	0.49250	0.51147	0.53439	0.55654	0.57678	0.59501	0.61137	0.62607	0.63934

if $\mu_1/\mu_2 < 5$, there are three roots; for greater ratio ($\mu_1/\mu_2 > 5$) the fourth root appears, which is significantly less than the first three. All the roots are real.

For a crack in a soft grain ($\mu_1/\mu_2 < 1$), the results are given in Table 12. In this case we have two closely located real roots, which grow slowly with decreasing μ_1/μ_2. The difference $\lambda_1 - \lambda_2$ between these roots is approximately constant when $\mu_1/\mu_2 < 0.3$.

Many other examples, examined by using the developed code, confirm the facts revealed above:

(i) the cases when there are more than one root in the strip $0 < \mathrm{Re}\,\lambda < 1$ are not rare;
(ii) quite commonly the roots are closely located.

These conclusions are important for the proper development of singular multi-wedge boundary elements.

4.3. Limits of applicability

Two factors, one geometrical and the other physical, influence the accuracy when tending to extreme values. The geometrical factor is the angle of a wedge: the system (7) degenerates when it tends to zero. The physical factor is the ratio of the shear moduli of successive wedges: when the ratio tends to zero or infinity, the system degenerates, as well. When these factors appear combined, as it occurs in a thin soft or rigid interface, one may expect drastic deterioration of the results. Thus, it is reasonable to study how the factors restrict the applicability of the method when they appear separately or combined.

The investigation has been carried out for the case, when a wedge with the angle Θ and the shear modulus μ_2 is embedded into a medium with the shear modulus μ_1 either in front of a crack tip, or in the medium without a crack. In both cases we use a simple analytical formulae to find the roots of the characteristic determinant what allows us to check the accuracy of the numerical results. To make checking reliable, we represent the embedding medium by a number of sub-wedges with the same properties. The number of the sub-wedges is taken five. As in the previous subsections, the accuracy of five significant digits is guaranteed when the values of the parameters Θ and μ_2/μ_1 are not extreme. We consider the accuracy deteriorating when the numerical results differ from those provided by the exact formula in the forth or less digit. The Poisson's ratio is taken the same for the wedge and embedding medium ($\nu_1 = \nu_2 = 0.3$).

4.3.1. Influence of the angle Θ

Consider the case of a thin wedge in front of a crack tip. Assume $\mu_2 = \mu_1$. Then we actually have a crack in a homogeneous medium; for its tip the exact value of the exponent is $\lambda = 0.5$. Numerical experiments for decreasing values of Θ gave this result with the accuracy of five significant digits when $\Theta > 1'$. For $\Theta = 1'$ we had $\lambda = 0.50001$; for $\Theta = 0.5'$ $\lambda = 0.5001$; $\Theta = 0.1'$ $\lambda = 0.503$. We conclude that the method is applicable to wedges with the angle up to first minutes when the shear modules do not differ significantly. This conclusion is confirmed below by the data for thin wedges when $\mu_2 \neq \mu_1$.

4.3.2. Influence of the ratio μ_2/μ_1

Consider the case of a wedge in a medium without a crack. Actually, we have a closed system of two wedges (Fig. 5a). Let the angle Θ be not small, equal, for certainty 7°. The calculations for μ_2/μ_1 tending to zero and infinity have shown that the accuracy of five digits holds even for $\mu_2/\mu_1 = 10^{-35}$ and 10^{35}, respectively. This means that the method is applicable to wedges with highly contrasting properties when their angles are not too small.

4.3.3. Combined influence of the angle Θ and the ratio μ_2/μ_1

The same closed system served us to investigate the combined influence of the parameters Θ and μ_2/μ_1. For a wedge with the angle 1°, there has been no loss of accuracy when $10^{-5} < \mu_2/\mu_1 < 10^8$. For a layer with the angle $\Theta = 9'$, the accuracy of five digits holds when $10^{-4} < \mu_2/\mu_1 < 10^7$. We conclude that the method is applicable to very thin wedges, both compliant and rigid. For such a wedge, one may apply an asymptotic approach (see, e. g. Mishuris and Kuhn, 2001), which represents the wedge by a single interface with an appropriate linear dependence between the displacement discontinuity and traction. Using the asymptotic approach suggests an easy extension of the method beyond the limits discussed in this subsection.

Acknowledgements

The authors gratefully acknowledge the support of the Russian Fund of Fundamental Researches (Grant No 03-05-64888). We thank Professor Gennady Mishuris for valuable discussions and comments, and Doctor Alana Selsil for the improvement of the manuscript. The first author is also grateful to the Mathematics Department of Rzeszow University of Technology for hospitality.

Appendix A. Distinct roots

For certainty, consider an open system with the tractions $\mathbf{p^0}$ and $\mathbf{p^n}$ prescribed at the external boundaries $i = 0$ and $i = n$, respectively. Then after substitution of (8) into Eq. (7), the latter become a system of $N = 2(n-1)$ equations for N unknown components of tractions at $n-1$ contacts. The determinant of the system is a holomorphic function of ρ, and is expanded into a convergent Taylor series in the vicinity of an arbitrary point ρ_*, such that,

$$D(\rho) = \sum_{s=0}^{\infty} a_s(\rho - \rho_*)^s, \tag{A.1}$$

where

$$a_s(\rho_*) = \frac{1}{s!}\left.\frac{\mathrm{d}^s D(\rho)}{\mathrm{d}\rho^s}\right|_{\rho=\rho_*}. \tag{A.2}$$

From (A.1) and (A.2) it is clear that if

$$D(\rho_*) = \left.\frac{\mathrm{d}D(\rho)}{\mathrm{d}\rho}\right|_{\rho=\rho_*} = \cdots = \left.\frac{\mathrm{d}^{k-1}D(\rho)}{\mathrm{d}\rho^{k-1}}\right|_{\rho=\rho_*} = 0, \tag{A.3}$$

then $\rho = \rho_*$ is a k-times repeated root of the characteristic Eq. (9). Since, for all the functions employed in this paper, we have $f(\bar{\rho}) = \overline{f(\rho)}$, then the conjugated value $\bar{\rho}_*$ is also a k-times repeated root of the characteristic Eq. (9). Finally, the pair ρ_* and $\bar{\rho}_*$, used when applying the residue theorem in the inversion (2), provides, as it must be, *real* physical values of stresses and displacements.

We first consider the case of a distinct root ρ_* ($k = 1$). The solution of (7) in Cramer's form is

$$x_s(\rho) = \frac{D_s(\rho)}{D(\rho)}, \tag{A.4}$$

where for an odd s, x_s is the normal component of the traction $x_s = p_1^j = \sigma_{\theta\theta}$ at the contact $j = (s+1)/2$, and for an even s, x_s is the shear component of the traction $x_s = p_2^j = \sigma_{r\theta}$ at the contact $j = s/2$. Also, $D_s(\rho)$ ($s = 1, \ldots, N$) are determinants defined by the Cramer's rule.

We have noted in Section 2.2 that the entries of the matrices in (7) are holomorphic functions in any finite region of the plane ρ. Hence, all the determinants $D_s(\rho)$ are holomorphic functions. Then all the components of the transformed tractions have a simple pole at the point $\rho = \rho_*$. By (3) and (4), the same refers to all components of stresses and displacements for any angle θ. As a result, the residue theorem applied to (2) gives terms of the form $\mathrm{Re}[A(\theta)r^{-(\rho+2)}]$ for physical stresses and terms of the form $\mathrm{Re}[B(\theta)r^{-(\rho+1)}]$ for physical displacements. There is no logarithmic multiplier in the asymptotic equations for physical values.

To further clarify the matter for a distinct root, we expand the matrices in (7) in series in $\Delta\rho = \rho - \rho_*$. Then, solving N Eq. (7), with prescribed and moved to the r.h.s. $\mathbf{p^0}$ and $\mathbf{p^n}$, by Jordan–Gauss elimination, we arrive at a system of the form:

$$\begin{pmatrix} 1\cdots 0 & a_{1,N} \\ \cdots & \cdots \\ 0\cdots 1 & a_{N-1,N} \\ 0\cdots 0 & \Delta\rho + 0(\Delta\rho^2) \end{pmatrix} \mathbf{P_N^*} = \mathbf{G_N}(\rho_*) + \mathbf{O}(\Delta\rho), \tag{A.5}$$

where $\mathbf{P_N^*}$ is a vector-column composed of N components of the vector $\mathbf{P_N} = (\mathbf{p^1}, \ldots, \mathbf{p^{n-1}})^{\mathrm{T}}$, which may differ, in order, from that of $\mathbf{P}_N$, due to the Jordan–Gauss procedure. The term $\mathbf{G_N}(\rho_*) = (g_1, g_2, \ldots, g_{2n-2})^{\mathrm{T}}$ is a vector-column, which linearly depends on $p^0_{\theta\theta}(\rho_*)$, $p^0_{r\theta}(\rho_*)$, $p^n_{\theta\theta}(\rho_*)$, $p^n_{r\theta}(\rho_*)$.

From the structure of (A.5), it is clear that only the term $g_{2n-2}/\Delta\rho$ will produce the pole of transformed tractions at $\rho = \rho_*$. Consequently, by (3) and (4), all the transformed stresses and displacements near the pole ρ_* will have the common multiplier $g_N/\Delta\rho$. Since ρ_* is a root of (9), the corresponding solution of the physical problem satisfies homogeneous contact conditions. Indeed, we will obtain the same results when considering the homogeneous system, that is,

$$\begin{pmatrix} 1\cdots 0 & a_{1,N} \\ \cdots & \cdots \\ 0\cdots 1 & a_{N-1,N} \\ 0\cdots 0 & 0 \end{pmatrix} \mathbf{P_N^*} = \mathbf{O_N},$$

where $\mathbf{O_N}$ is the zero vector-column $N \times 1$. The last (zero) row corresponds to a free variable. By setting it equal to $g_{2n-2}(\rho_*)/\Delta\rho$, we arrive at the same solution.

We now recall that in computations for an applied problem, the prescribed distributions of tractions $\mathbf{p^0}$ and $\mathbf{p^n}$ on the outer boundaries are arbitrary. Hence, the real and imaginary parts of $g_N(\rho_*)$ may be considered as arbitrary constants to be used in approximations of stresses and displacements near a singular point. These constants are called the stress intensity factors (SIF). If a distinct root ρ_* is real, then $g_N(\rho_*)$ is also real, and hence, a single SIF corresponds to a real distinct root of (9).

Appendix B. Repeated roots

Under some combination of wedge angles, elastic properties and types of boundary conditions, repeated roots of (9) may appear. The most well-known example is a traction-free crack in a homogeneous medium: in this particular case, the root $\rho_* = -3/2$ of (9) is *repeated twice*, while the corresponding poles are *distinct*, resulting in two well-known SIFs. This simplest case may serve to clarify general features of systems with repeated roots.

Indeed, consider an open system composed of two similar wedges (Fig. B1). In this case $\Theta^1 = \Theta^2 = \Theta$, $\mu^1 = \mu^2 = \mu$, $k^1 = k^2 = k$. For the only contact, $i = 1$, Eq. (7), written for a homogeneous case ($\mathbf{p^0} = \mathbf{p^2} = \mathbf{0}$), become:

$$\begin{pmatrix} a_{11} & 0 \\ 0 & a_{22} \end{pmatrix} \begin{pmatrix} p^1_{\theta\theta} \\ p^1_{r\theta} \end{pmatrix} = \begin{pmatrix} 0 \\ 0 \end{pmatrix},$$

where $a_{11} = (\rho+1)\sin 2\Theta + \sin[(\rho+1)2\Theta]$, $a_{22} = (\rho+1)\sin 2\Theta - \sin[(\rho+1)2\Theta]$; as expected, these coefficients correspond to T^S and T^A, respectively, for a single wedge with the angle 2Θ.

The determinant is $D(\rho) = a_{11}a_{22}$, and the characteristic equation

$$D(\rho) = 0 \tag{B.1}$$

is satisfied when: (i) $a_{11} \neq 0$ or $a_{22} \neq 0$; (ii) $a_{11} = a_{22} = 0$. It is easy to see that if $\Theta \neq \pi/2, \pi$ then the roots of (B.1) are distinct ($a_{11} + a_{22} \neq 0$). Then either $p^1_{\theta\theta}$ (for $a_{11} = 0$), or $p^1_{r\theta}$ (for $a_{22} = 0$) is an arbitrary constant. Thus we have a single SIF.

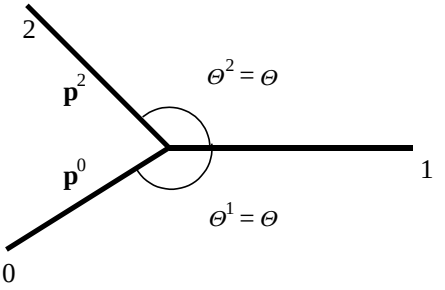

Fig. B1. An open system composed of two similar wedges.

When $\Theta = \pi/2$, the system of the two wedges represents a half-plane. The root $\rho_* = -2$ is repeated twice. In this case, $a_{11} = 0$, $a_{22} = 0$ and both $p^1_{\theta\theta}$ and $p^1_{r\theta}$ are free constants. The corresponding exponent for stresses $-(\rho_* + 2)$ is equal to zero, and these two 'SIFs' do not produce singularities in stresses, when the external tractions are assumed to be continuous.

When $\Theta = \pi$, the system represents a plane with a crack. For this case, the root is $\rho_* = -3/2$. It is repeated twice. Again $a_{11} = 0$, $a_{22} = 0$ and both $p^1_{\theta\theta}$ and $p^1_{r\theta}$ are arbitrary, i.e. we have two free constants. The corresponding poles of the solution are distinct. Indeed, the expansion of a_{11} and a_{22} in $\Delta\rho = \rho - \rho_*$, similar to that used in Appendix A, gives the following representation:

$$2\pi\begin{pmatrix} \Delta\rho + \mathrm{O}(\Delta\rho^2) & 0 \\ 0 & \Delta\rho + \mathrm{O}(\Delta\rho^2) \end{pmatrix}\begin{pmatrix} p^1_{\theta\theta} \\ p^1_{r\theta} \end{pmatrix} = \begin{pmatrix} g_1(\rho_*) \\ g_2(\rho_*) \end{pmatrix} + \mathrm{O}(\Delta\rho^2). \tag{B.2}$$

From (B.2) we see that, although the expansion (A.1) of the determinant $D(\rho)$ starts with the second degree of $\Delta\rho$ ($a_1 = 0$, $a_2 = 4\pi^2 \neq 0$), the solution $p^1_{\theta\theta}$, $p^1_{r\theta}$ has the pole $\rho_* = -3/2$ of the first degree, which is a distinct pole. There are two well-known SIFs corresponding to the free constants $p^1_{\theta\theta}$ and $p^1_{r\theta}$.

Note that, to have a pole of the second degree, the resulting matrix in the process of the Jordan–Gauss elimination must be of the form

$$\begin{pmatrix} 1 & a_{12} \\ 0 & \Delta\rho^2 \end{pmatrix}$$

with the term $\Delta\rho^2$ as an element of the main diagonal. From the residue theorem it follows that this term generates a logarithmic multiplier to the common exponential singularity in stresses, i.e. $(\ln r)r^{-(\rho_*+2)}$.

Now consider an arbitrary open system when the root is repeated k times ($k > 1$). According to (A.1)–(A.3), this occurs when the determinant $D(\rho)$ and its derivatives, up to the order $k - 1$, are zero at $\rho = \rho_*$. The expansion (A.1) starts from the term a_k:

$$D(\rho) = \sum_{s=k}^{\infty} a_s \Delta\rho^s, \tag{B.3}$$

where

$$a_s(\rho_*) = \frac{1}{s!}\left.\frac{\mathrm{d}^s D(\rho)}{\mathrm{d}\rho^s}\right|_{\rho=\rho_*}, \tag{B.4}$$

$$D(\rho_*) = \left.\frac{\mathrm{d}D(\rho)}{\mathrm{d}\rho}\right|_{\rho=\rho_*} = \cdots = \left.\frac{\mathrm{d}^{k-1}D(\rho)}{\mathrm{d}\rho^{k-1}}\right|_{\rho=\rho_*} = 0, \quad \left.\frac{\mathrm{d}^k D(\rho)}{\mathrm{d}\rho^k}\right|_{\rho=\rho_*} \neq 0. \tag{B.5}$$

We denote by m the rank of the system at $\rho = \rho_*$. The Gauss–Jordan elimination does not influence the rank. Hence, after expanding the matrix in $\Delta\rho = \rho - \rho_*$, and applying the elimination, the product of the terms of the main diagonal must be of the order $\Delta\rho^k$. Consequently, the resulting matrix will be of the form:

$$l \leqslant k \text{ rows} \quad \begin{pmatrix} \dots & \dots & \dots & \dots & \dots & \dots \\ 0 & \dots & 1 & a_{N-l,N+1-l} & \dots & a_{N-l,N} \\ 0 & \dots & 0 & \Delta\rho^{s_1} + \mathrm{O}(\Delta\rho^{s_1+1}) & \dots & a_{N+1-l,N} \\ \dots & \dots & \dots & \dots & \dots & \dots \\ 0 & \dots & 0 & 0 & \dots & \Delta\rho^{s_l} + \mathrm{O}(\Delta\rho^{s_l+1}) \end{pmatrix}, \tag{B.6}$$

where

$$l = N - m \leqslant k, \quad s_1 + \cdots + s_l = k. \tag{B.7}$$

From the first of (B.6) it is obvious that $m \geqslant N - k$. Two cases are possible:

(i) $m = N - k$. For this case $l = k$, and the second of (B.6) implies that each of the last l rows contains $\Delta\rho$ only at the first degree. This means that the pole $\rho = \rho_*$ is simple for each component of the solution (A.4). Then the residue theorem, applied to inversion (2), shows that the physical values do not contain a logarithmic multiplier to the common exponential asymptotics. The only difference with the case of a distinct root is that now we have at least two SIFs, even for a real root. The case of a crack considered above serves as an illustration.

(ii) $m > N - k$. For this case $l < k$, and at least one of s_i is greater than 1. Consequently, the corresponding transformed traction defined by (A.4) has a pole of the degree exceeding 1. Then the residue theorem, applied to inversion (2), gives a logarithmic multiplier, in addition to the common exponential multiplier.

Thus, we have proved the theorem:

Theorem. *The necessary and sufficient conditions for asymptotic stresses to have a logarithmic multiplier, generated by a root of (9) are*

$$k > 1, \quad m > N - k, \tag{B.8}$$

where N is the order of the matrix, m is its rank, and k is the degree of a root defined by (B.4).

This theorem enhances the result by Dempsey and Sinclair (1979). These authors proved that the *necessary* conditions are

$$D(\rho_*) = \left.\frac{\mathrm{d}D(\rho)}{\mathrm{d}\rho}\right|_{\rho=\rho_*} = \cdots = \left.\frac{\mathrm{d}^{N-m}D(\rho)}{\mathrm{d}\rho^{N-m}}\right|_{\rho=\rho_*} = 0. \tag{B.9}$$

Comparing (B.8) with (B.4) shows that $k - 1 \geqslant N - m$, that is, $m \geqslant N - k + 1 > N - k$. Since at the root we have $m < N$, the inequality $k - 1 \geqslant N - m$ implies $k > 1$. Thus, (B.8) is equivalent to the conditions (B.7). Consequently, these conditions are not only necessary but also *sufficient* to have a logarithmic multiplier.

With the physical multi-wedge systems, two questions arise:

(i) Can the rank m be greater than $N - k$? In other words, may a logarithmic multiplier to the common exponential behaviour of stresses appear?

(ii) Can the rank m be equal to $N - k$ when $k > 2$. In other words, is possible to have more than two SIFs for a multi-wedge system?

The answer to the first question is positive. It follows from the examples of purely logarithmic singularities summarized in Sinclair (1999) for the case of a single wedge (in our notation, the purely logarithmic singularity corresponds to the repeated root $\rho_* = -2$, that is $\lambda = 0$).

Presently, we do not have a theory allowing us to answer the second question. In our computations for various multi-wedge systems we have never had examples, which give positive answer to the question (ii). Perhaps, this is due to the extreme rarity of repeated roots, especially roots repeated more than twice. We doubt whether they are possible, in principle: it is difficult to imagine a system of elastic wedges having more than two SIFs for the same root. A similar conclusion is presented in Sinclair (1999) for a single wedge. In his study,

Sinclair used a matrix of the fourth order and question (ii) is reformulated as follows: can the rank be less than two? The author concludes (p. 560): "In the analysis of all the configurations... the ranks of the coefficient matrices involved never drop below two." In the footnote on the same page he comments: "It is difficult to see how the rank can be less than 2 in any further problem...". Our discussion above gives a means to check numerically the options for an arbitrary system by evaluating the rank in each particular case.

References

Blinova, V.G., Linkov, A.M., 1995. A method to find asymptotic forms at the common apex of elastic wedges. J. Appl. Math. Mech. 59, 187–195 (Transl. Prikl. Mat. Mekh., 1995, 59, 199–208).

Bogy, D.B., 1968. Edge-bonded dissimilar orthogonal elastic wedges under normal and shear loading. J. Appl. Mech. 35, 460–466.

Bogy, D.B., 1971. Two edge-bonded elastic wedges of different materials and wedge angles under surface tractions. J. Appl. Mech. 38, 377–386.

Chen, D.-H., Nisitani, H., 1993. Singular stress field near the corner of jointed dissimilar materials. J. Appl. Mech. 60, 607–613.

Comninou, M., 1977. Interface crack with friction in the contact zone. J. Appl. Mech. 44, 780–781.

Cook, T.S., Erdogan, F., 1972. Stresses in bonded materials with a crack perpendicular to the interface. Int. J. Eng. Sci. 10, 677–697.

Dempsey, J.P., 1981. The wedge subjected to tractions: a paradox resolved. J. Elast. 11, 1–10.

Dempsey, J.P., 1995. Power-logarithmic stress singularities at bi-material corners and interface cracks. J. Adhes. Sci. Technol. 9, 253–265.

Dempsey, J.P., Sinclair, G.B., 1979. On the stress singularities in the plane elasticity of the composite wedge. J. Elast. 9, 373–391.

Dobroskok, A.A., Ghassemi, A., Linkov, A.M., 2005. Extended structural criterion for numerical simulation of crack propagation and coalescence under compressive loads. Int. J. Fracture 133, 223–246.

Dundurs, J., 1969. Discussion of edge-bonded dissimilar orthogonal elastic wedges under normal and shear loading. J. Appl. Mech. 36, 650–652.

Dundurs, J., Lee, M.S., 1972. Stress concentration at a sharp edge in contact problems. J. Elast. 2, 109–112.

Dyskin, A.V., 1997. Crack growth criteria incorporating non-singular stresses: size effect in apparent fracture toughness. Int. J. Fracture 83, 191–206.

Erdogan, F., Gupta, G.D., 1975. The inclusion problem with a crack crossing the boundary. Int. J. Fracture 11, 13–27.

Hein, V.L., Erdogan, F., 1971. Stress singularities in a two-material wedge. Int. J. Fracture Mech. 7, 317–330.

Kalandia, A.I., 1969. Remarks on the singularity of elastic solutions near corners. Prikl. Mat. Mekh. 33, 127–131.

Kolk, K., Kuhn, G., Mishuris, G., 2003. 3D singularities with application to fatigue crack growth. In: Movchan, A.B. (Ed.), Proc. IUTAM Symposium "Asymptotics, Singularities and Homogenization in Problems of Mechanics". Kluwer Academic Publishers, pp. 477–486.

Korn, G.A., Korn, T.M., 2000. Mathematical Handbook for Scientists and Engineers, second ed. Dover, New York.

Leblond, J.B., Frelat, J., 2000. Crack kinking from an initially closed, ordinary or interface crack, in the presence of friction. Eng. Fracture Mech. 71, 289–307.

Linkov, A.M., Koshelev, V.F., Blinova, V.G., 2002. Tip, corner and wedge elements: a regular way to increase accuracy of the BEM. Proc. Int. Conference IABEM 2002. Kinkas (Ed.), Austin, USA (CD-ROM).

Mishuris, G., Kuhn, G., 2001. Comparative study of an interface crack for different wedge-interface models. Arch. Appl. Mech. 71, 764–780.

Munz, D., 2004. Stresses and fracture in joints. ESIS Newsletters, European Structural Integrity Soc. 40, 31–37.

Murakami, Y. (Ed.), 1990. Handbook. Stress Intensity Factors, vols. 1, 2. Pergamon Press, Oxford-New York.

Neuber, H., 1946. Theory of Notch Stresses. J.W. Edwards, Ann Arbor, Michigan.

Nicaise, S., Sändig, A.-M., 1999. Transmission problem for the Laplace and elasticity operators: regularity and boundary integral formulation. Math. Methods Appl. Sci. 9, 855–898.

Noda, N.-A., Takase, Y., Hamashima, T., 2003. Generalized stress intensity factors in the interaction within a rectangular array of rectangular inclusions. Arch. Appl. Mech. 73, 311–322.

Novozhilov, V.V., 1969. On a necessary and sufficient criterion for brittle strength. J. Appl. Math. Mech. 33, 201–210.

Rao, A.K., 1971. Stress concentration and singularities at interface corners. Z. Angew. Math. Mech. 51, 395–406.

Seweryn, A., 1994. Brittle fracture criterion for structure with sharp notches. Eng. Fracture Mech. 47, 673–681.

Seweryn, A., 2003. Metody Numericzne w Mechanice Pęcania. Biblioteka Mechaniki Stosowanej. Polska Academia Nauk. Institut Podstawowych Problemov Techniki. Warszawa (in Polish).

Seweryn, A., Mroz, Z., 1995. A non-local stress failure condition for structural elements under multiaxial loading. Eng. Fracture Mech. 51, 955–973.

Seweryn, A., Molski, K., 1996. Elastic stress singularities and corresponding generalized stress intensity factors for angular corners under various boundary conditions. Eng. Fracture Mech. 55, 529–556.

Sinclair, G.B., 1998. Further paradoxes in generalized Levy problems. J. Elast. 50, 253–259.

Sinclair, G.B., 1999. Logarithmic stress singularities resulting from various boundary conditions in angular corners of plates in extension. J. Appl. Mech. 66, 556–560.

Theocaris, P.S., 1974. The order of singularity at multi-wedge corner of a composite plate. Int. J. Eng. Sci. 12, 107–120.

Tranter, C.J., 1948. The use of Mellin trnsform in finding the stress distribution in an infinite wedge. Quart. J. Mech. Appl. Math. 1,2, 125–130.

Wang, W.-C., Chen, J.-T., 1994. Singularities of an arbitrary inclined semi-infinite crack meeting a bimaterial interface. Eng. Fracture Mech. 49, 671–680.

Williams, M.L., 1952. Stress singularities resulting from various boundary conditions in angular corners of plates in extension. J. Appl. Mech. 19, 526–528.

Williams, M.L., 1956. The complex-variable approach to stress singularities—II. J. Appl. Mech. 23, 477–478.